Electronic Supplementary Information

Magnetic nanoparticles containing soft-hard diblock copolymer films with high order

Senlin Xia[a], Lin Song[a], Volker Körstgens[a], Matthias Opel[b], Matthias Schwartzkopf[c], Stephan V. Roth[c,d], Peter Müller-Buschbaum[a],*

[a]Technische Universität München, Physik-Department, Lehrstuhl für Funktionelle Materialien, James-Franck-Straße 1, 85748 Garching, Germany

[b]Walther-Meissner-Institut, Bayerische Akademie der Wissenschaften, Walther-Meissner-Str. 8, 85748 Garching, Germany

[c]Deutsches Elektronen-Synchrotron DESY, Notkestrasse 85, 22603 Hamburg, Germany

[d]KTH Royal Institute of Technology, Department of Fibre and Polymer Technology, Teknikringen 56-58, SE-100 44 Stockholm, Sweden

Email: muellerb@ph.tum.de

Experimental Details

Optical Microscopy (OM)

OM images were measured via an Axiolab A microscope (Carl Zeiss) equipped with five different magnifications and combined with a PixeLink USB Capture BE 2.6 charge coupled device (CCD) camera. Films were probed at various magnifications.

Atomic Force Microscopy (AFM)

AFM measurements were done with a JSPM-5200 AFM (Jeol) in tapping mode at ambient conditions. The employed tip had a curvature radius of less than 15 nm and was positioned onto cantilevers (ULTRASHARP NSC35/ALBS, MikroMasch) with a spring constant of 7.5 N/m and a resonance frequency of 170 kHz. All AFM data were processed and analyzed by the software WinSPM v2.14.

Scanning Electron Microscopy (SEM)

A NVision40 FESEM by Carl Zeiss AG was employed for SEM measurements with accelerating voltages of 1.5 and 5 kV, at working distances of 1.7 and 3.5 mm, respectively. To confirm the sample homogeneity, SEM measurements were performed on each sample in many randomly selected spots, located in the four corners and in the center of the rectangular samples.

Power spectral density (PSD) from SEM images

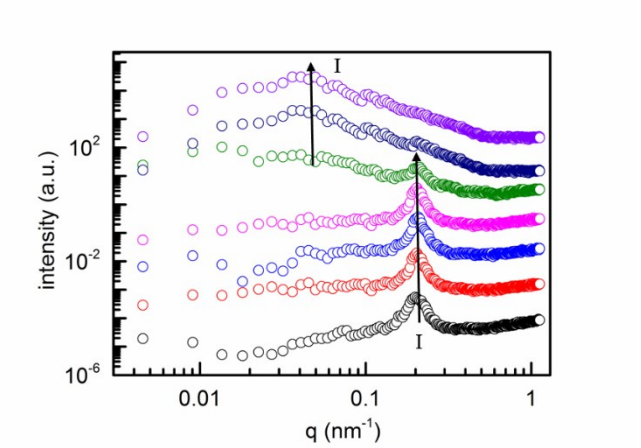

Figure S1. Power spectral density (PSD) functions extracted from azimuthal integration of the intensity distribution in the FFT patterns with different NP concentrations: 0, 0.5, 1, 2, 5, 7, and 10 wt %, from bottom to top. Peak I shows the q value of the lateral structure originated from microphase separation of the DBC. The PSD profiles are shifted for clarity along y axis.

AFM topography images

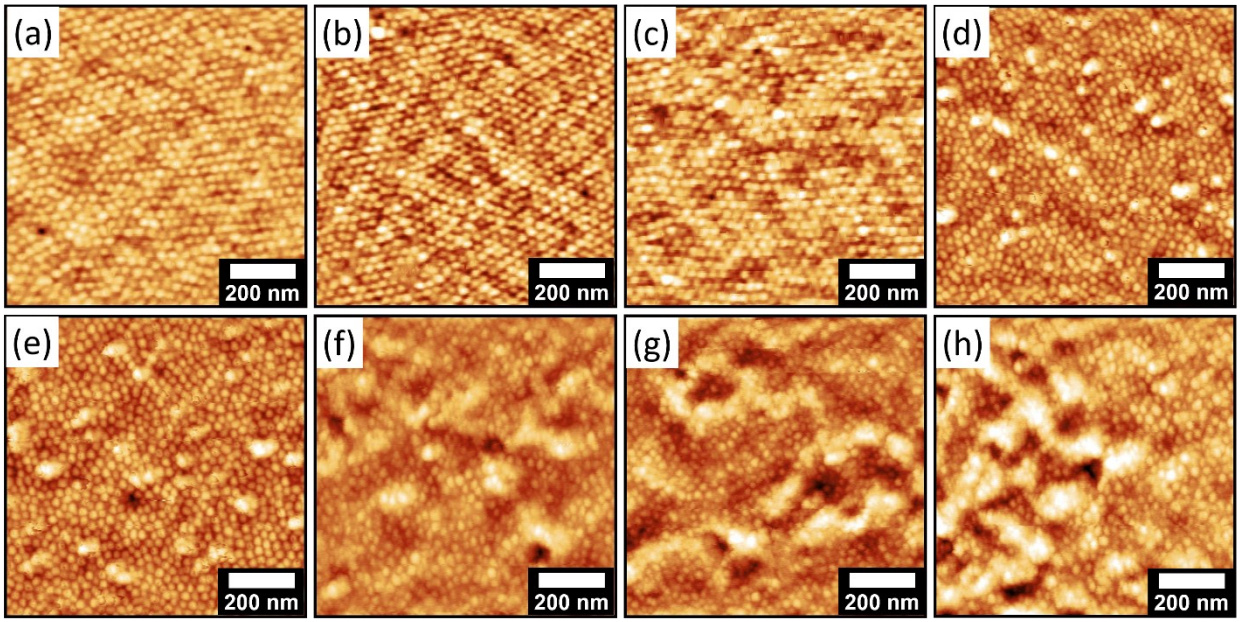

Figure S2. AFM topography images of the printed hybrid films at various NP concentrations: (a) 0, (b) 0.5, (c) 1, (d) 2, (e) 5, (f) 7, (g) 10 and (h) 20 %.

For all AFM images, bright areas and dark areas correspond to the PS and PNIPAM areas, respectively. At low NP concentrations, the order of the cylindrical domains increases with increasing loading of NP, whereas, the further addition of NPs at high concentrations perturbs the order. At considerable high NP concentration (≥ 10 wt%), there are substantial NP aggregates, forming irregular sizes and accumulating randomly on the film surface instead of following the alignment of the PS domains from the DBC template (Figure S2f-h). Because the NP clusters cannot be further accommodated inside the PS cylindrical domains, the localization of the NPs is no longer correlated with the DBC template and structures are deformed.

Composition of film surface

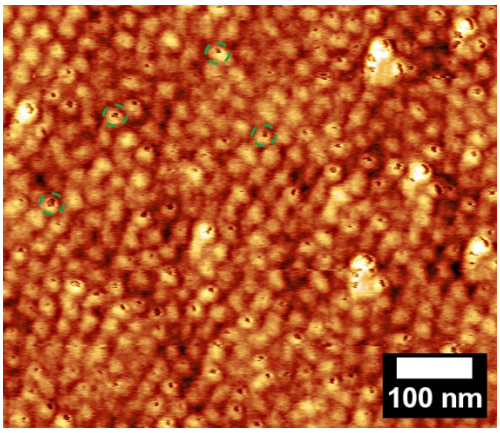

Figure S3. AFM topography image of hybrid film containing 1 wt % of NPs. Green dashed circles show the NPs located inside the PS domains.

From the above AFM image (Figure S3), one can clearly see that the hybrid film surface is heterogenerously composed of PNIPAM (dark yellow part), PS (bright yellow part) and NPs (white part). Additionally, one can also observe dark dots (shown as green dashed circles) located inside the bright yellow PS domains. This is due to the stiffness of NPs, and can also evidences the presence of NPs inside PS blocks.

Quantitative information on structure order

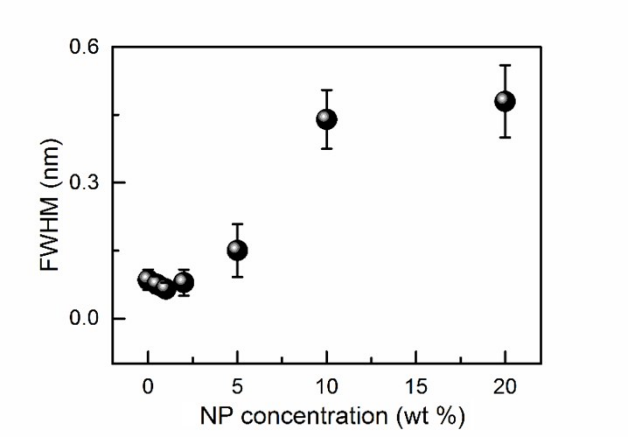

Figure S4. Values of the full width at half maximum (FWHM) of the peak II at q_y =0.228 nm^{-1} as a function of NP concentration. Data are extracted from fitting the horizontal line cuts.

Comparison of magnetic data

temperature	data source	$B_{c//}$ / $B_{c\perp}$	$M_{r//}$ / $M_{r\perp}$
5K	literature	2.36	1.82
	our work	1.08	1.21
100K	literature	1.57	1.18
	our work	1.02	1.04

Table S1. Comparison of magnetic data between our work and literature.[1] $B_{c//}$ and $B_{c\perp}$ are the magnetic coercivity in the orientation with the magnetic field parallel and vertical to the NP wires, respectively. $M_{r//}$ and $M_{r\perp}$ are remenance measured with NP wires parallel and vertical to the magnetic field.

A comparison is made between our work and that from another group, in which numerical values of magnetic data are provided. In the literature,[1] the authors used a magnetic field to direct the arrangement of the magnetic NPs (Fe_3O_4) and to obtained NP wires showing a magnetic anisotropy. The comparison is detailed in Table S1. From the table, one can see that a similar magnetic anisotropy behavior is observed. For both investigations, a higher magnetic coercivity (B_c) and remenance (M_r) are obtained in the orientation with NP wires parallel to the magnetic field. However, literature reports a higher B_c increment at both temperatures, while similar B_c values are observed in both orientation (also seen in Figure 13). This means that only similar fields are needed to erase the film's magnetic memory created in both orientations. Such difference could be attributed to factors, such as the nature of magnetic NPs, the size and size distribution of NPs and NP wires as well as the film homogeneity.

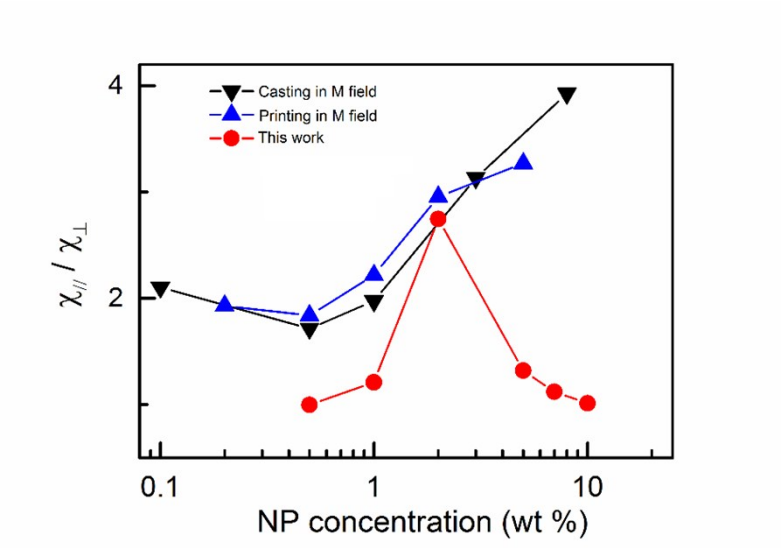

Figure S5. Comparison of magnetic anisotropy present in films fabricated via different methods (with and without magnetic field). Red circles are the data of the present work, in which solvent vapor annealing is employed without any magnetic field. Blue and black triangles are data of films prepared within magnetic field via printing[2] and solution casting[3], respectively. The magnetic susceptibility in both parallel ($\chi_{//}$) and perpendicular ($\chi_{\perp}$) orientation (with respect to the NP-wires) are obtained from a linear fit at zero field area. The susceptibility ratio $\chi_{//} / \chi_{\perp}$ is calculated and plotted versus NP concentrations. Lines are guides to the eyes.

In our previous work, a magnetic field was employed to guide the NPs alignment during the film deposition (based on printing[2] and on solution casting[3]). The final films (thickness above 1 μm) contained macroscale NP-wires, which resulted in higher absolute values of the magnetic susceptibility as compared with the present study. To characterize the different responsive behavior in both orientations, the magnetic susceptibility ratio $\chi_{//} /\chi_{\perp}$ is calculated. From Figure S5, one can see that the magnetic anisotropy obtained at 2 wt % in the present work is comparable with our previous investigations, which suggests the field free film fabrication method in the present work is very promising.

1. Y. Sahoo, M. cheon, S. Wang, H. Luo, E. P. Furlani, P. N. Prasad. *J. Phys. Chem. B*, **2004**, 108, 3380-3383.
2. S. L. Xia, E. Metwalli, M. Opel, P. A. Staniec, E. M. Herzig and P. Müller-Buschbaum, *Acs. Appl. Mater. Inter*, 2018, **10**, 2982-2991.
3. Y. Yao, E. Metwalli, M. A. Niedermeier, M. Opel, C. Lin, J. Ning, J. Perlich, S. V. Roth and P. Müller-Buschbaum, *Acs. Appl. Mater. Inter*, 2014, **6**, 5244-5254.